



Removal of Textile Dye using Carbon Nanotubes as an Adsorbent in Fixed Bed Column

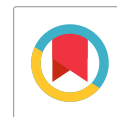
S. Karthikeyan^{1*}, C. Amudha², S. Tamilselvi², K. Gopal²

¹Department of Chemistry, Chikkanna Government Arts College, Tiruppur, TN, India

²Department of Chemistry, Erode Arts and Science College, Erode, TN, India

Received: 10.02.2016 Accepted: 20.05.2016 Published: 30-06-2016

*environkarthi@gmail.com



ABSTRACT

In this present study, we used Carbon Nanotubes (CNT) as an adsorbent for the removal of Acid Blue dye. MWNTs are synthesized from *Rosmarinus officinalis* oil as a Non-conventional precursor on to Fe/Mo catalyst supported on silica at 50 °C under N₂ atmosphere by spray pyrolysis process. The efficiency of the CNT has been detected by the fixed bed column Adsorption studies with various parameters like initial dye concentration, different flow rate and bed height. The down-flow column adsorption technique is used to assessing the stability of the chosen adsorbent for design purpose. The Bed Depth Service Time (BDST), Thomas and Yoon-Nelson Models were applied for the analysis of Acid Blue dye adsorption in the column.

Keywords: Adsorbate; Adsorbent; Fixed bed column; HRTEM.

1. INTRODUCTION

Adsorption is the preferential partitioning of substances from the vaporish or liquid part on to the surface of a solid's substrate. The method of sorption involves separation of substance from one part in the course of accumulation or concentration at the surface of another. The adsorbing phase is the adsorbent and the material concentrated or adsorbed at the surface of that phase is the adsorbate. The adsorption results in the formation of a monolayer of the adsorbate on the surface of the adsorbent (Karthikeyan *et al.* 2012). The sorption applications of CNT to tackle environmental pollution problems have received considerable attention in which CNT used as fixed bed, continuous flow through this bed result in maximum utilization of the adsorption capacity. For the application of the CNT as adsorbents in fixed bed column experiments, different parameters need to be optimized, such as flow rate, the bed thickness and diameters and initial concentration of the pollutant.

For example, MWCNT/alumina nanocomposite as sorbent has been reported to be an effective for the removal of lead ions from aqueous solution with pH range of 3-7. The efficiency of the sorbent has been tested in batch mode and fixed bed, column mode. It has been reported that by increasing agitation speed, contact time and adsorbent dosage the amount of the removal is increased. CNT-iron oxides magnetic composites has been successfully applied as adsorbent for removal of different targets from water such as Pb(II) (Li *et al.* 2005), Cu(II) (Lee *et al.* 2001), Ni(II) (Kandah and Meunier, 2007) and Sr(II) (Chen *et al.* 2009).

2. COLUMN STUDIES

In the continuous flow method, the solution is allowed to pass through a stationary fixed bed of the adsorbent. During the initial stages of operation, the adsorbate species readily adsorb on the first few layers of the adsorbent effectively. These first few layers have contact with the solution containing maximum amount of the solute. During the subsequent flow of the influent, the adsorbate species, escaping adsorption from the first few layers, adsorb on the subsequent layers. This zone is practically saturated with respect to the adsorbate species and hence, this zone cannot adsorb further. In column studies, it is necessary to note the importance of the term break through point. The term break point or break through point refers to the volume of the influent passed through the bed before reaching maximum effluent concentration and beyond the break through point, the adsorbent can adsorb only very little amount of the adsorbate.

The break through point increases with the increase in the bed depth. The break through point increases with the decrease in the flow rate (Karthikeyan *et al.* 2014). The break through point increases with the decrease in the initial concentration of the influent.

The Adsorbent containing diameter of 50-100 nm and length of 5-10 μm was used for the study. A glass wool column of diameter 2.5 cm was used. Clean glass wool was placed at the bottom and top of the column to retain the carbon and prevent disturbance of the bed by high flow rates. Slurry of the adsorbent was prepared

with distilled water and slowly transferred in to the column. After complete transfer of the adsorbent, bed was washed with distilled water. Dye solution under study was placed in a reservoir. The Experimental Setup for the fixed bed column is given in Fig. 1.

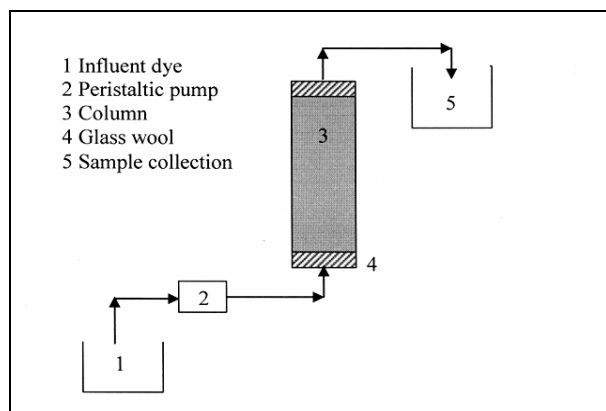


Fig. 1: Fixed bed column experimental setup

2.1 Adsorbate

Acid Blue dye solution is prepared by dissolving accurately weighed dyes in distilled water at respective concentration. The concentration of dye solution was determined using a spectrophotometer operating in the visible range on absorbance. The Structure of Acid Blue dye molecule is given in Fig. 2. The summary data including the color index is given in Table 1.

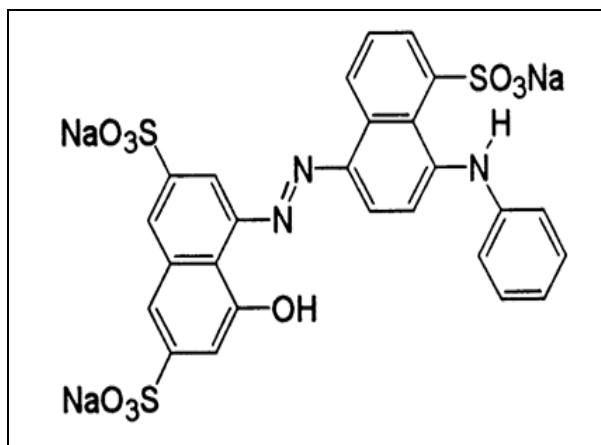


Fig. 2: Structure of acid blue dye

Table 1. Summary data on dye studied

Generic Name	Classification	Color Index	Class
Blue	Anionic	62125	Acid

2.2 CNT as an Adsorbent

The CNT provides chemically inert surfaces with high specific surface areas for physical adsorption. They have relatively uniform structure, providing more adsorption sites. Adsorbent used for this study is Multi-walled carbon nanotubes (MWNTs), which have been synthesized by simple method of spray pyrolysis using *Rosmarinus officinalis* oil on Fe/Mo catalyst supported on silica under nitrogen atmosphere. CNTs as an adsorbent media able to remove wide range of contaminant heavy metals such as Cr^{3+} (Di *et al.* 2006), Pb^{2+} (Li *et al.* 2005) and Zn^{2+} (Purnachandra *et al.* 2007), metalloids such as arsenic compounds (Peng *et al.* 2005), organics such as polycyclic aromatic organic compounds (Gotovac *et al.* 2007; Hedderman *et al.* 2006; Yang *et al.* 2006), atrazine (Yan *et al.* 2008) and a range of biological contaminants including bacteria (Akasaka and Watari, 2009; Deng *et al.* 2008; Srivatsava *et al.* 2004; Upadhyayula *et al.* 2008; Upadhyayula *et al.* 2009), viruses (Brady-Estevéz *et al.* 2008; Mostafavi *et al.* 2009), NOM (Hyung and Kim, 2008; Lu and Su, 2007; Saleh *et al.* 2008; Su and Lu, 2007) and cyanobacterial toxins (Albuquerque *et al.* 2008; Yan *et al.* 2004; Yan *et al.* 2006). Nanosorbents such as CNTs, polymeric materials (e.g. dendrimers), zeolites have exceptional adsorption properties and are applied for removal of heavy metals, organics and other impurities (Savage and Diallo, 2005). Adsorption of metal contaminants and organics on CNT is widely studied and extensively reviewed (Purnachandra Rao *et al.* 2007).

3. VARIOUS MODELS FOR BED COLUMN STUDY

3.1 Bed Depth Service Time (BDST) Model

BDST model states that the bed height and service time of a column bear a linear relationship. This model was derived based on the assumption that forces like intra particle diffusion and external mass transfer resistance are negligible and that the adsorbate is adsorbed onto the adsorbent surface directly. This model is used only for the description of the initial part of the breakthrough curve (i.e.) up to the breakpoint or 10–50% of the saturation points (Kundu and Gupta, 2006).

The original BDST model was carried out by Bohart and Adams and given in Equation (1).

$$\ln \left(\frac{C_0}{C_B} - 1 \right) = \ln \left(\exp \left[\frac{KXN_0}{V} \right] - 1 \right) - KC_0 t \quad (1)$$

A linear relationship between bed depth and service time is given by eq. (2)

The straight line represent as:

$$t = \frac{N_0 X}{C_0 V} - \frac{1}{C_0 K} \ln\left(\frac{C_0}{C_B} - 1\right) \quad (2)$$

Where, 'a' is the intercept of BDST line $a = \left(\frac{N_0}{V C_0}\right)$ and the slope of this equation represented as eq. (3).

$$b = \frac{1}{K C_0} \ln\left(\frac{C_0}{C_B} - 1\right) \quad (3)$$

Thus, N_0 and k can be evaluated from slope (a) and the intercept (b) of the plot of t versus X , respectively. The critical bed depth (X_0) is the theoretical depth of adsorbent sufficient to ensure that the outlet solute concentration does not exceed the breakthrough concentration (C_B) value at time $t = 0$.

3.2 Thomas Model

Among the Thomas (1948) model is simple to use in the design of a fixed-bed adsorption column. Therefore the break through data obtained from the column studies was examined using the kinetic model developed by Thomas (1948). The expression of the Thomas model for an adsorption column is as follows.

$$C_0/C_t = 1/\{1 + \exp[k/Q(N_0 M - C_0 V)]\} \quad (4)$$

Where,

- C_t = effluent dye concentration, mg/L
- C_0 = initial dye concentration, mg/L
- K = Thomas rate constant L /min. mg
- N_0 = maximum dye adsorption capacity, mg/g
- M = mass of the carbon, g
- V = throughput volume of the dye solution, mL
- Q = flow rate, mL/min

Equation (4) can be converted to the simple format as follows:

$$C_t/C_0 = 1/[\exp(b-aV)] \quad (5)$$

Where,

$$a = K C_0 / Q \quad (6)$$

$$b = K N_0 M / Q \quad (7)$$

Therefore if Q , M and C_0 are constants, C_t/C_0 is the function of V . Once a & b are determined the value of K & N_0 can be calculated from eq. 6 & 7.

3.3 Yoon-Nelson Model

This model was developed by Yoon and Nelson in 1984 to describe the adsorption breakthrough curves. The Yoon-Nelson model was derived based on the assumption that the rate of decrease in the probability of adsorption for each adsorbate molecule is proportional to the probability of adsorbate adsorption and the

probability of adsorbate breakthrough on the adsorbent. This model that requires no detailed data concerning the type of the adsorbent and the physical properties of the adsorption bed (Aksu and Gonen, 2004; Chowdhury et al. 2013). The linearised model for a single component system is expressed as:

$$\ln\left(\frac{C_0}{C_0 - C_t}\right) = K_{YN} t - \mathcal{T} K_{YN} \quad (8)$$

Where, K_{YN} is the rate constant (min^{-1})

\mathcal{T} is the time required for 50% adsorbate breakthrough (min)

t is the breakthrough time (min)

The values of K_{YN} and \mathcal{T} can be calculated from a plot of $\ln\left(\frac{C_0}{C_0 - C_t}\right)$ vs. t at different inlet concentrations, flow rates and bed heights. If the theoretical model accurately characterizes the experimental data, this plot will result in a straight line with a slope of K_{YN} and intercept of $\mathcal{T} K_{YN}$ (Yoon and Nelson, 1984).

4. MATERIALS & METHODS

4.1 Preparation of Catalyst

The preparation of Fe/Mo catalyst was conducted using wet impregnation method. $\text{Fe}(\text{NO}_3)_3 \cdot 9\text{H}_2\text{O}$ and $\text{NH}_4\text{Mo}_7\text{O}_{24} \cdot 4\text{H}_2\text{O}$ were dissolved in methanol and mixed thoroughly with methanol suspension of silica. The solvent was then evaporated and the resultant cake heated to 90-100 °C for 3 hours, removed from the furnace and ground in a mortar. The fine powders were then calcined for 1 hour at 450 °C and then re-ground before loading into the reactor.

4.2 Synthesis of MWNTs

The catalyst was placed on the quartz boat. The boat was placed in the heating furnace. The carrier gas nitrogen (100 mL/min) was flushed out before switch on the reaction furnace to remove air and create nitrogen atmosphere. The temperature was raised from room temperature up to the desired growing temperature. Waiting was done for 10 min for stabilization of temperature. Synthesis was conducted at 650 °C in nitrogen atmosphere, with a typical reaction time of 30 min. *Rosmarinus officinalis* oil were supplied at a rate of 0.1 g/min. The reactor was then allowed to cool to room temperature with nitrogen gas flowing. The carbon product on the silica support was then weighed to determine the carbon yield. We define carbon yield here as the functional mass as $(m_1 - m_0)/m_0$, where m_1 and m_0 are the final mass and the initial mass of the catalyst support with carbon deposit respectively.

4.3 Purification of MWNTs

The MWNTs were purified by 40 mg of raw material was added to 20 mL 1N HCl to form an acidic slurry. This slurry was heated to 60 °C and stirred at 600 rpm. To this heated acidic slurry 20 mL H₂O₂ was added to form oxidative slurry that continued to be heated and stirred for 30 minutes. The addition of HCl, H₂O₂, subsequent heating and stirring was repeated three more times, each time allowing the heated oxidative slurry to stir for 30 min. Phase separation was allowed to proceed followed by filtering the carbon phase and washing with 1N HCl and distilled water. The collected sample was dried at 120 °C in air for 2 hrs. The morphology of the sample was characterized by SEM, HRTEM and Raman spectroscopy.

5. APPLICABILITY OF FIXED BED COLUMN MODELS

Fig. 3 is the Scanning Electron Microscopy (SEM) image of the as-grown nanostructures over Fe-Mo bimetallic catalyst, impregnated in silica at 650 °C under the flow of nitrogen by CVD assisted spray pyrolysis method. SEM image clearly reveals that MWNTs grew nicely on the surface of the silica particles.

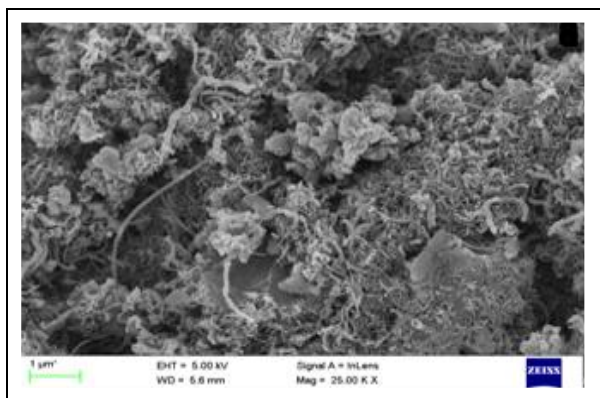


Fig. 3: SEM images of MWNTs grown Fe-Mo supported on silica at 650 °C

In fig. 4, we have presented the high resolution HRTEM images of MWNTs, grown over Fe-Mo bimetallic catalyst impregnated on silica support at 650 °C with a flow rate of *Rosmarinus officinalis* oil at 0.5 mL per minute. That the inner diameters of the nanotubes were in the range of 4-6 nm and the outer diameters of the grown nanotubes found in the range of 16-18 nm. The wall and inner core are clearly visible in fig. 4.

The results of Raman spectroscopy analysis in Fig. 5 represents the MWNTs grown on the catalyst surface at 650 °C, indicating two characteristic peaks at 1354 cm⁻¹ and 1582 cm⁻¹ which correspond to D and G bands, respectively. The G bands are associated with stretching vibration within the basal plane of graphite

crystal that is normalized to an equivalent intensity. The D bands are associated with the disorder or defective planar graphite structure. The D peaks at 1354 cm⁻¹ may be attributed to the defects in the curved graphene sheets. Therefore, the Raman spectrum provides definite proof that the MWNTs have graphitic structure.

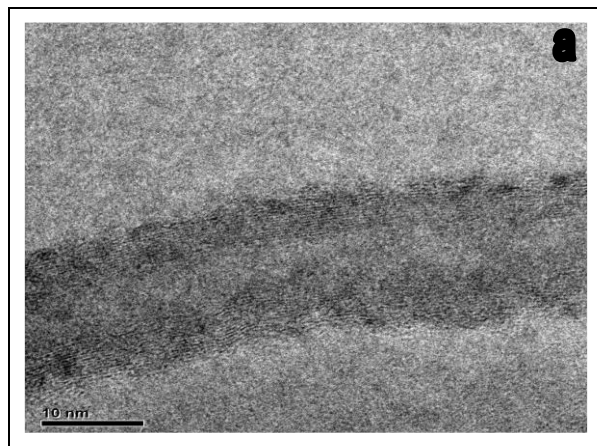


Fig. 4: HRTEM images of MWNTs grown Fe-Mo supported on silica at 650 °C

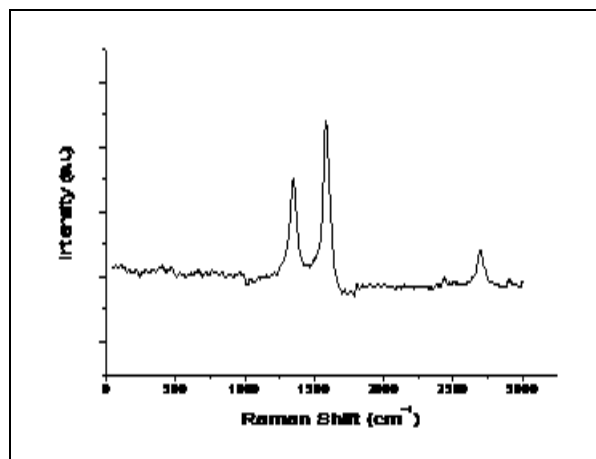


Fig. 5: Raman spectrum of grown MWCNTs at 650 °C

5.1 Applicability of BDST Model

If an adsorbate-adsorbent system obeys BDST model, a linear trace is expected for a plot of $\ln \left[\frac{C_0}{C_t} - 1 \right]$ vs. Time. Where, C_0 and C_t is initial effluent dye concentration and concentration of effluent at time t , respectively. The column experiments were conducted with a view to examine the influence of initial dye concentration on the chosen dye adsorbed by MWNTs on the adsorption capacity of the adsorbent.

The Fig. 6 represents the relation between C_t/C_0 and volume of the effluent, which gives a typical S shaped curve confirming the applicability of the BDST model for Acid Blue. Fig. 7 represent the relationship between $\ln \left[\frac{C_0}{C_t} - 1 \right]$ and time.

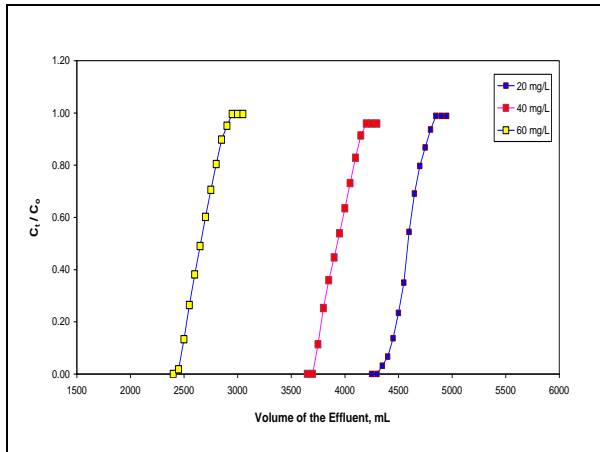


Fig. 6: Effect of initial dye concentration on break through curve for acid blue

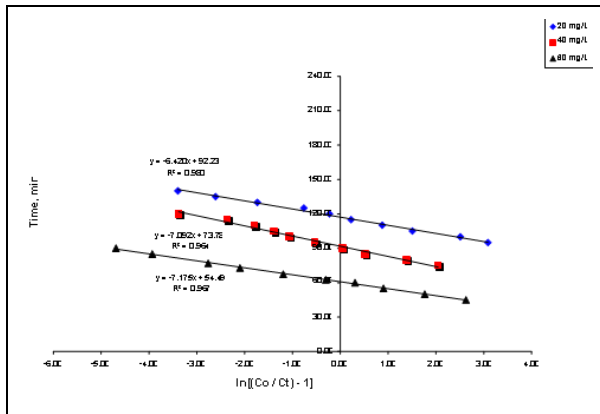


Fig. 7: Effect of initial dye concentration on BDST model for acid blue

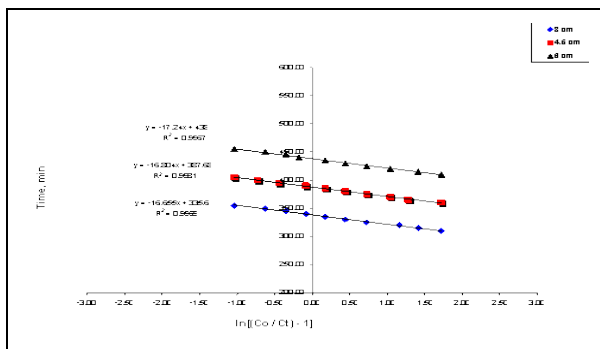


Fig. 8: Effect of bed height on BDST model for acid blue

The experiments were conducted with a view to examine the influence of bed height on the individual dye adsorption. The respective plots for the BDST model under approximately same experimental condition with

different Bed heights viz., 3.0 cm, 4.5 cm and 6.0 cm were drawn and these are shown in the respective Fig. 8. The influences of flow rate at different of initial dye concentration solution of Acid Blue on the adsorptive capacity through the BDST model was examined.

The Fig. 9 represents the variation of $\ln[(C_0/C_t) - 1]$ with time for three different flow rate Viz., 10, 20 & 30 mL/min.

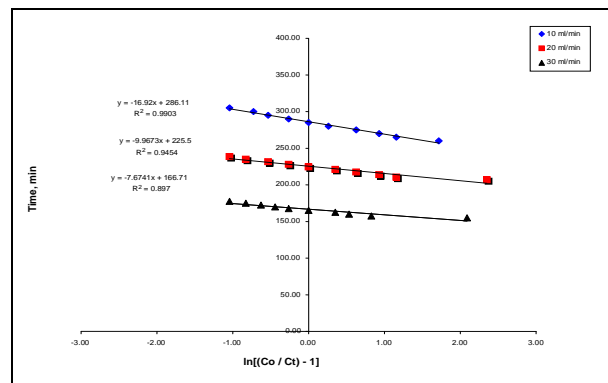


Fig. 9: Effect of flow rate on BDST model for acid blue

5.2 Applicability of Thomas Model

If a adsorbate – adsorbent system obeys Thomas model, a linear trace is expected for a plot of Volume of the effluent Vs $\ln[C_0/C_t - 1]$. Where, C_0 and C_t is initial effluent dye concentration and concentration of effluent at time, t, respectively. The experiments were conducted with a view to examine the Initial dye concentration, influence of bed height and influence of flow rate on the individual dye adsorption on the chosen adsorbate adsorption. The Fig. 10 to 12 confirms applicability of Thomas model.

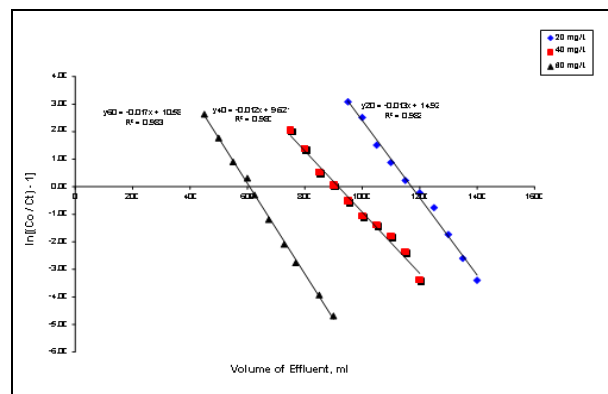


Fig. 10: Effect of initial dye concentration on Thomas model for acid blue

Table 2. Influence of initial dye concentration, bed height and flow rate on BDST, Thomas and Yoon-Nelson models parameters

Parameters	Values	BDST Model		Thomas Model		Yoon-Nelson Model	
		K L/Mg.Min	No Mg/G	K L/Mg.Min	No Mg/G	K _{yn} L/Min	T/Mg/G
Dye Con, Mg/L	20	0.155	27.66	6.5×10 ⁻³	11,476	0.140	117.28
	40	0.141	22.13	3.1×10 ⁻³	15,517	0.145	96.48
	60	0.139	16.34	2.8×10 ⁻³	18,892	0.164	62.81
Bed Height	3	0.060	100.68	1.7×10 ⁻³	69,114	0.059	343.22
	4.5	0.059	174.42	1.2×10 ⁻³	61,386	0.059	390.16
	6	0.058	262.8	1.1×10 ⁻³	52,100	0.059	398.47
Flow Rate	10	0.059	85.83	1.2 ×10 ⁻³	63,320	0.055	287.81
	20	0.100	33.82	4.5 ×10 ⁻³	47,555	0.059	224.93
	30	0.130	16.67	8.2 ×10 ⁻³	36,543	0.066	178.33

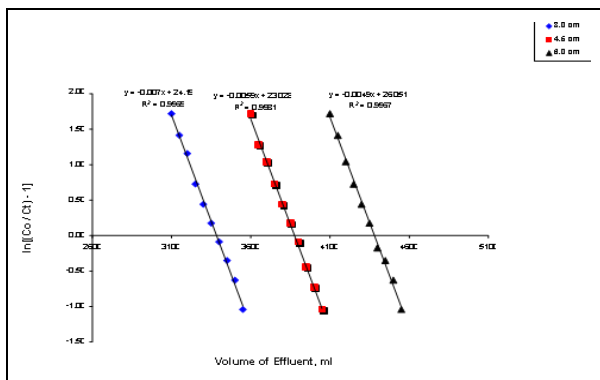


Fig. 11: Effect of bed height on Thomas model for acid blue

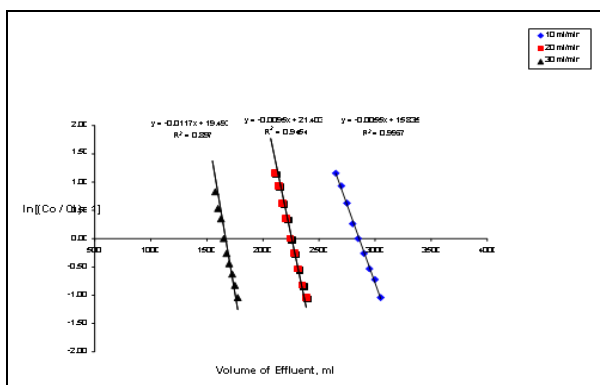


Fig. 12: Effect of flow rate on Thomas model for acid blue

5.3 Applicability of Yoon-Nelson Model

If an adsorbent-adsorbate obeys Yoon-Nelson model a linear trace is expected. For a plot of Time Vs $\ln[C_0/C_t - C_t]$. Where, C_0 and C_t is initial effluent dye concentration and concentration of effluent at time ‘t’ respectively. The experiments were conducted with a view to examine the Initial dye concentration, influence of bed height and influence of flow rate on the individual

dye adsorption. Fig. 13 to 15 confirm applicability of Yoon- Nelson model.

The values of adsorptive capacity (N_0) obtained from each model indicates that initial dye concentration has same significant of the adsorptive capacity. Hence increases initial dye concentration increases the adsorption capacity. It is evident from the result that the capacity per gram is higher only for lower bed height values hence, splitting into many beds enhance.

The rate of flow has considerable influents on dye removal, when the flow rate low the break through volume is high. The adsorptive capacity of MWNTs obtained fixed bed experiment for each model where higher than that of the value obtained by batch type experiments. It is evident from results that the rate of flow has considerable on the influents on dye removal when the flow rate is low, the breakthrough volume is high the slow flow rate is more effective compared with fast flow rate.

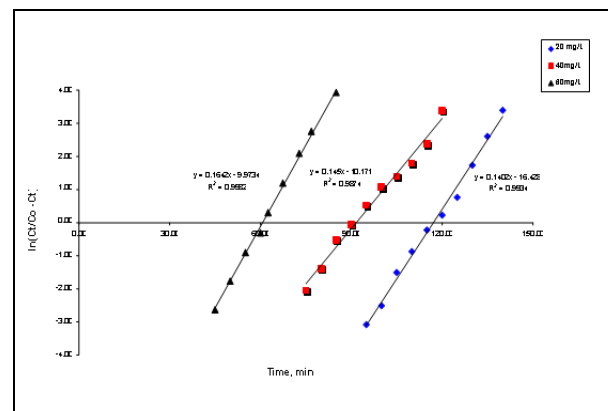


Fig. 13: Effect of initial dye concentration on Yoon & Nelson model for acid blue

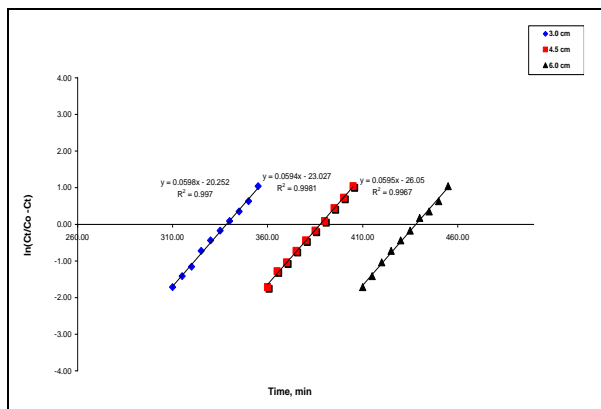


Fig. 14: Effect of bed height on Yoon & Nelson model for acid blue

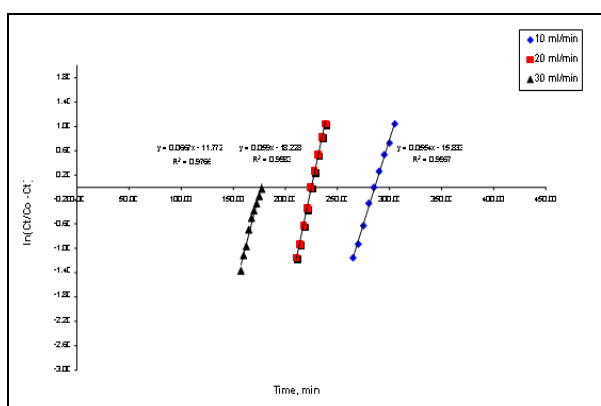


Fig. 15: Effect of flow rate on Yoon & Nelson model for acid blue

The adsorption capacity calculated based on BDST model has good agreement with the adsorbed value high R^2 value. Whereas adsorption capacity calculated by Thomas and Yoon-Nelson model shows poor correlation co-efficient. In general the BDST model describes adsorption capacity behaviour of Acid Blue onto chosen adsorbent column more responsibility than Thomas and Yoon-Nelson model out of three model tested the chosen adsorbent- adsorbate system fits exceptionally well with BDST model with good coefficient of determination.

FUNDING

This research received no specific grant from any funding agency in the public, commercial, or not-for-profit sectors.

CONFLICTS OF INTEREST

The authors declare that there is no conflict of interest.

COPYRIGHT

This article is an open access article distributed under the terms and conditions of the Creative Commons Attribution (CC-BY) license (<http://creativecommons.org/licenses/by/4.0/>).



6. CONCLUSION

The literature survey has revealed only very little onsite onto the applicability and viability of the adsorption techniques using a low cost Nano structured Carbon material as an adsorbent. The result of the present work are summarized that the BDST model is found to be successfully applicable to the chosen adsorbate-adsorbent system. The results are in good agreement with the fact that the service time increases with the bed depth. The N_0 values for Thomas, BDST and Yoon-Nelson models were determined & these values are reported. The Thomas modal equation is found to be successfully applicable to the chosen adsorbate-adsorbent system indicating that the conclusions, obtained from the study of the applicability of the BDST modal, are true. The column studies for the removal of chosen dye from aqueous solution indicated different performances, depended upon the dye structure. For acid blue, the CNTs in the column proposed the highest adsorption capacity.

REFERENCES

- Akasaka, T. and Watari, F., Capture of bacteria by flexible carbon nanotubes, *Acta Biomater.*, 5(2), 607-612(2009). <https://doi.org/10.1016/j.actbio.2008.08.014>
- Aksu, Z. and Gönen, F., Biosorption of phenol by immobilized activated sludge in a continuous packed bed: Prediction of breakthrough curves, *Process Biochem.*, 39(5), 599-613(2004). [https://doi.org/10.1016/S0032-9592\(03\)00132-8](https://doi.org/10.1016/S0032-9592(03)00132-8)
- Brady-Estevéz, A. S., Kang, S. and Elimelech, M., A single walled carbon nanotube filter for removal of viral and bacterial pathogens, *Small*, 4(4), 481-484(2008). <https://doi.org/10.1002/sml.200700863>
- Changlun Chen, Jun Hu, Dadong Shao, Jiaying Li and Xiangke Wang, Adsorption behavior of multiwall carbon nanotube/iron oxide magnetic composites for Ni(II) and Sr(II), *J. Hazard. Mater.*, 164(2-3), 923-928(2009). <https://doi.org/10.1016/j.jhazmat.2008.08.089>
- Chowdhury, Z., Zain, S., Rashid, A., Rafique, R. and Khalid, K., Breakthrough curve analysis for column dynamics sorption of Mn(II) ions from wastewater by using Mangostana garcinia peel-based granular-activated carbon, *J. Chem.*, 2013, 8(2013). <https://doi.org/10.1155/2013/959761>

- Delgado, L. F., Charles, P., Glucina, K. and Morlay, C., The removal of endocrine disrupting compounds, pharmaceutically activated compounds and cyanobacterial toxins during drinking water preparation using activated carbon-A review, *Sci. Total. Environ.*, 435-436, 509-525(2012).
<https://doi.org/10.1016/j.scitotenv.2012.07.046>
- Deng, S. D. S., Upadhyayula, V. K. K., Smith, G. B. and Mitchell, M. C., Adsorption Equilibrium and Kinetics of Microorganisms on Single-Wall Carbon Nanotubes, *IEEE Sens. J.*, 8(6), 954-962(2008).
<https://doi.org/10.1109/JSEN.2008.923929>
- Di, Z. C., Ding, J., Peng, X. J., Li, Y. H., Luan, Z. K. and Liang, J., Chromium adsorption by aligned carbon nanotubes supported ceria nanoparticles., *Chemosphere*, 62(5), 861-865(2006).
<https://doi.org/10.1016/j.chemosphere.2004.06.044>
- Gotovac, S., Yang, C. M., Hattori, Y., Takahashi, K., Kanoh, H. and Kaneko, K., Adsorption of polyaromatic hydrocarbons on single wall carbon nanotubes of different functionalities and diameters, *J. Colloid. Interface. Sci.*, 314(1), 18-24(2007).
<https://doi.org/10.1016/j.jcis.2007.04.080>
- Hedderman, T. G., Keogh, S. M., Chambers, G. and Byrne, H. J., In-depth study into the interaction of single walled carbon nanotubes with anthracene and p-terphenyl, *J. Phys. Chem. B.*, 110(9), 3895-3901(2006).
<https://doi.org/10.1021/jp055647q>
- Hyung, H. and Kim, J. H., Natural organic matter (NOM) adsorption to multi-walled carbon nanotubes: Effect of NOM characteristics and water quality parameters, *Environ. Sci. Technol.*, 42(12), 4416-4421(2008).
<https://doi.org/10.1021/es702916h>
- Kandah, M. I. and Meunier, J. L., Removal of nickel ions from water by multi-walled carbon nanotubes, *J. Hazard. Mater.*, 146(1-2), 283-288(2007).
<https://doi.org/10.1016/j.jhazmat.2006.12.019>
- Karthikeyan, S. and Sivakumar, P., The effect of activating agents on the activated carbon prepared from *Feronia limonia* (L.) swingle (wood apple) shell, *J. Environ. Nanotechnol.*, 1(1), 5-12(2012).
<https://doi.org/10.13074/jent.2012.10.121009>
- Karthikeyan, S., Santhi, P., Saravanan, A. and Saranya, K., Sorption of basic dye (Rhodamine B) by Nano porous activated carbon from *Sterculia Quadrifida* shell waste, *J. Environ. Nanotechnol.*, 3(1), 88-100(2014).
<https://doi.org/10.13074/jent.2013.12.132087>
- Kundu, S. and Gupta, A. K., Arsenic adsorption onto iron oxide-coated cement (IOCC): Regression analysis of equilibrium data with several isotherm models and their optimization, *Chem. Eng. J.*, 122(1), 93-106(2006).
<https://doi.org/10.1016/j.cej.2006.06.002>
- Lee, S. M. and Davis, A. P., Removal of Cu(II) and Cd(II) from aqueous solution by seafood processing waste sludge, *Water Res.*, 35(2), 534-540(2001).
[https://doi.org/10.1016/S0043-1354\(00\)00284-0](https://doi.org/10.1016/S0043-1354(00)00284-0)
- Li, Y. H., Di, Z., Ding, J., Wu, D., Luan, Z. and Zhu, Y., Adsorption thermodynamic, kinetic and desorption studies of Pb²⁺ on carbon nanotubes, *Water Res.*, 39(4), 605-609(2005).
<https://doi.org/10.1016/j.watres.2004.11.004>
- Lu, C. and Su, F., Adsorption of natural organic matter by carbon nanotubes, *Sep. Purif. Technol.*, 58(1), 113-121(2007).
<https://doi.org/10.1016/j.seppur.2007.07.036>
- Mostafavi, S. T., Mehrnia, M. R. and Rashidi, A. M., Preparation of nanofilter from carbon nanotubes for application in virus removal from water, *Desalination*, 238(1-3), 271-280(2009).
<https://doi.org/10.1016/j.desal.2008.02.018>
- Peng, X., Luan, Z., Ding, J., Di, Z., Li, Y. and Tian, B., Ceria nanoparticles supported on carbon nanotubes for the removal of arsenate from water, *Mater Lett.*, 59(4), 399-403(2005).
<https://doi.org/10.1016/j.matlet.2004.05.090>
- Rao, G. P., Lu, C. and Su, F., Sorption of divalent metal ions from aqueous solution by carbon nanotubes: A review, *Sep. Purif. Technol.*, 58(1), 224-231(2007).
<https://doi.org/10.1016/j.seppur.2006.12.006>
- Savage, N. and Diallo, M. S., Nanomaterials and water purification: Opportunities and challenges, *J. Nanopart. Res.*, 7, 331-342(2005).
<https://doi.org/10.1007/s11051-005-7523-5>
- Srivastava, A., Srivastava, O. N., Talapatra, S., Vajtai, R. and Ajayan, P. M., Carbon nanotube filters, *Nat. Mater.*, 3(9), 610-614(2004).
<https://doi.org/10.1038/nmat1192>
- Su, F. and Lu, C., Adsorption kinetics, thermodynamics and desorption of natural dissolved organic matter by multiwalled carbon nanotubes, *J. Environ. Sci. Heal.*, 42(11), 1543-1552(2007).
<https://doi.org/10.1080/10934520701513381>
- Upadhyayula, V. K. K., Deng, S., Mitchell, M. C., Smith, G. B., Nair, V. K. and Ghoshroy, S., Adsorption kinetics of Escherichia coli and Staphylococcus aureus on single-walled carbon nanotube aggregates, *Water Sci. Technol.*, 58(1), 179-184(2008).
<https://doi.org/10.2166/wst.2008.634>
- Upadhyayula, V. K. K., Deng, S., Smith, G. B. and Mitchell, M. C., Adsorption of Bacillus subtilis on single-walled carbon nanotube aggregates, activated carbon and NanoCeram, *Water Res.*, 43(1), 148-156(2009).
<https://doi.org/10.1016/j.watres.2008.09.023>
- Yan, H., Gong, A., He, H., Zhou, J., Wei, Y. and Lv, L., Adsorption of microcystins by carbon nanotubes, *Chemosphere*, 62(1), 142-148(2006).
<https://doi.org/10.1016/j.chemosphere.2005.03.075>
- Yan, H., Pan, G., Zou, H., Li, X. L. and Chen, H., Effective removal of microcystins using carbon nanotubes embedded with bacteria, *Chinese Sci. Bull.*, 49(16), 1694-1698(2004).
<https://doi.org/10.1007/BF03184300>
- Yan, X. M., Shi, B. Y., Lu, J. J., Feng, C. H., Wang, D. S. and Tang, H. X., Adsorption and desorption of atrazine on carbon nanotubes, *J. Colloid. Interface Sci.*, 321(1), 30-38(2008).
<https://doi.org/10.1016/j.jcis.2008.01.047>
- Yang, K., Zhu, L. and Xing, B., Adsorption of Polycyclic Aromatic Hydrocarbons by Carbon Nanomaterials, *Environ. Sci. Technol.*, 40(6), 1855-1861(2006).
<https://doi.org/10.1021/es052208w>
- Yoon, Y. H. and Nelson, J. H., Application of gas adsorption kinetics, I. A theoretical model for respirator cartridge service life, *Am. Ind. Hyg. Assoc. J.*, 45(8), 509-516(1984).
<https://doi.org/10.1080/15298668491400197>